

Small scale systems of galaxies. I. Photometric and spectroscopic properties of members¹

L. Tanvuia

Institut für Astronomie, Universität Wien, Türkenschanzstraße 17, A-1180 Wien, Austria

`tanvuia@astro.univie.ac.at`

B. Kelm, P. Focardi

Dipartimento di Astronomia, Università di Bologna, Via Bertini Pichat 6, Bologna, Italy

`kelm@bo.astro.it, focardi@bo.astro.it`

R. Rampazzo

INAF - Osservatorio Astronomico di Padova, Vicolo dell'Osservatorio 5, I-35122, Padova, Italy

`rampazzo@pd.astro.it`

and

W.W. Zeilinger

Institut für Astronomie, Universität Wien, Türkenschanzstraße 17, A-1180 Wien, Austria

`zeilinger@astro.univie.ac.at`

ABSTRACT

This paper is the first of a series addressed to the investigation of galaxy formation/evolution in small scale systems of galaxies (SSSGs) which are located in low density cosmic environments. Our algorithm for SSSG selection, includes galaxy systems of 2 or more galaxies lying within $\Delta cz \leq 1000 \text{ km s}^{-1}$ and a $200 h_{100}^{-1} \text{ kpc}$ radius volume. We present the analysis of the photometric and spectroscopic properties of 19 member galaxies belonging to a sample of 11 SSSGs.

In the $\mu_e - r_e$ plane, early-type members may be considered “ordinary”, not “bright” galaxies in the definition given by Capaccioli et al. (1992) with a significant fraction of galaxies having a disk or disk-like isophotes. We do not detect

fine structure and signatures of recent interaction events in the early-type galaxy population, a picture also confirmed by the spectroscopy.

At odd, there are several spiral members with open arm configurations as expected in interacting systems. At the same time, emission lines in the spectra of spiral members fall in the HII regions regime defined with diagnostic diagrams (Veilleux & Osterbrock 1987). None of the objects displays unambiguous indication of nuclear activity, although four spiral nuclei could be ascribed to the class of Seyferts. The star formation rate seems enhanced over the average expected in spiral galaxies only for poorer SSSGs in particular pairs ($\leq 50 M_{\odot} \text{ yr}^{-1}$) but without being in the range of starburst systems.

Subject headings: Galaxies: distances and redshifts; Galaxies: photometry; Galaxies: spectroscopy; Galaxies: interactions

1. Introduction

Among cosmic environments, small scale systems of galaxies (SSSGs) in the field are those in which not only galaxy–galaxy interactions but also the evolution of cosmic structures can be studied at a “cellular” level. To the SSSG class of cosmic structure we may ascribe galaxy systems with different richness and density characteristics spanning from compact groups to poorer configurations like galaxy pairs.

Together with compact galaxy groups (Hickson 1997, and references therein), investigated in definitely more detail, recent X-ray observations suggest the physical reality of some loose groups (Ponman et al. 1996; Mulchaey 2000) and even pairs (Henricksen & Cousineau 1999; Trinchieri & Rampazzo 2001). The X-ray diffuse component and the plethora of faint galaxies associated to the few dominant members is interpreted as due to the presence of a deep potential well (Mulchaey 2000).

Are then SSSGs long lasting associations or, in the hierarchical evolution scenario, the debris of older, richer and sparse configurations? Are pairs the debris of a pristine group and consequently a way station toward isolated Es? NGC 1132, an isolated elliptical with extended X-ray diffuse emission (Mulchaey & Zabludoff 1999), could be a prototypical example of the evolution of such systems. Some scenarios (Diaferio et al. 1994; Governato,

¹Based on observations obtained at the European Southern Observatory, La Silla, Chile (Programme Nr. 57.B–036)

Tozzi & Cavaliere 1996) depict rich and compact galaxy structures, like Hickson compact groups, as substructures of larger ones, with different degree of equilibrium. Zabludoff & Mulchaey (1998) found typically 20 to 50 dwarf galaxies associated to their X-ray detected groups. In this context, SSSGs of different richness and degree of compactness have to be studied comparatively as “single” class of cosmic environments.

The understanding of galaxy–galaxy interaction phases and the evolution of cosmic structures are deeply interconnected. Galaxy encounters in SSSGs are less frequent than in galaxy clusters, but the low velocity dispersion of the SSSG may lead to efficient merging episodes (Barnes 1996). Interactions could severely alter the properties of a galaxy up to modify the original morphological class (Barnes 1996; Kennicutt 1996) and then re-direct the evolution of a galaxy triggering various phenomena ranging from star formation (Longhetti et al. 1999) to galaxy activity (Monaco et al. 1994; Rafanelli, Violato & Baruffolo 1995; Laurikainen & Salo 1995; Keel 1996; Kelm, Focardi & Palumbo 1998; Coziol et al. 2000). In this picture, the environment plays a key role since it dictates the predominant type of encounters (Moore et al. 1996; Barnes 1996). A connection should then exist between the local environment and the global properties of galaxies inhabiting it. For rich galaxy systems, many aspects of the connection between environment and galaxy properties have emerged, from radio (Haynes, Giovanelli & Chincarini 1984) to X-ray properties (Forman & Jones 1982). The link between the environment and the galaxy evolution in SSSGs is still not fully understood (Ponman et al. 1996; Longhetti et al. 1998a,b, 1999, 2000; Rampazzo et al. 2000; Mulchaey 2000; Coziol et al. 2000) and partly suffers a shortage of information with respect to richer environments.

In order to understand which parameters dominate in galaxy interactions, we started a study of SSSGs, defined in 3D redshift space. SSSGs have been selected in a low density environment, i.e. they appear as overdense systems with respect to the average galaxy distribution.

The present paper collects photometric and spectrophotometric data for the main members of a sample of SSSGs. Within the picture described above, dominant galaxies in SSSG have potentially the power of revealing the history and evolutionary phase of the respective SSSGs. Elliptical galaxies may be at the center of the potential well of a SSSG as suggested by X-ray observations (Mulchaey 2000) and could present fine structures (Schweizer 1996) reminiscent of past interaction events. Spiral galaxies in mixed pairs could be the last undigested member of a pre-existing group (Rampazzo & Sulentic 1992) and could reveal their on-going interaction not only through morphological distortion but also in their possibly triggered activity.

The goals of the present paper are the following: 1) to obtain a redshift estimate which

will provide an independent check of the systemic velocities of the SSSG members typically made available by large redshift surveys, 2) to investigate the structure of the member galaxies through a detailed surface photometry, 3) to analyze the possible induced activity using medium resolution spectroscopy and diagnostic models.

The paper is organized as follows: The sample is defined in § 2. A description of the photometric and spectroscopic observations, data reduction and analysis is given in § 3, while results of individual objects are presented in § 4. The global morphological, photometric and spectroscopic properties of the present sample as a function of the SSSG and SSSG member properties are discussed in § 5.

2. The sample definition

The SSSG sample includes 11 systems of 2 or more galaxies lying at similar redshift ($\Delta cz \leq 1000$ km/s) and within a $200 h^{-1}$ kpc radius area, for which new spectroscopic or photometric data have been acquired.

These confirmed SSSGs constitute a small subset of a SSSGs candidate sample which includes likely misclassified isolated galaxies in ZCAT (Huchra et al. 1992). The version of ZCAT used for selection of candidates contains 57536 entries. The SSSGs candidate sample was selected with a two-step procedure: first, isolated galaxies were identified in ZCAT with an automatic code defining as isolated all those galaxies presenting no neighbour(s) with known redshift within $\Delta cz \pm 1000$ km/s and $\Delta R = 1h^{-1}$ Mpc. With this procedure, 3890 galaxies were selected in the redshift interval $3000 < cz < 10000$ km s $^{-1}$ out of a sample of 18677 galaxies in total. ZCAT is essentially a redshift compilation rather than a complete sample and also includes a $\approx 25\%$ fraction of galaxies with unknown redshift, Therefore, many of the selected isolated galaxies presented one or more projected companion(s), and are therefore likely misclassified isolated galaxies. To account for this, the code has identified, in the second step, among the isolated galaxies, those presenting nearby projected neighbours (i.e. neighbours whose redshift is unknown), which are clearly likely to represent in fact small scale galaxy systems. This resulted in 423 candidate SSSGs.

All candidates lying within 1 Abell radius and $\Delta cz \leq 1000$ km/s from ACO clusters (Struble & Rood 1999) have been excluded from the sample. We have also inspected DSS images to select among the projected pairs and groups those appearing outside clusters and dense large groups, and are consequently suited for photometric and spectral inspection. Once systems inside clusters are rejected one can safely assume the SSSG sample includes only systems in low density environment. However, we expect that SSSGs reside in environ-

ments not as sparse as those typically associated to single galaxies, based on the result by Focardi & Kelm (2002), showing (in their figure 10) that compact groups display a significant excess of neighbours with respect to galaxies lacking a close neighbour.

The sample of galaxy systems we present here is very small: it covers a large range in radial velocity and absolute magnitude, and is partially based on catalogues that are not complete. Further it has been defined making also use of non-automatic selection criteria, causing an intrinsic and hardly quantifiable bias. Therefore, we do not expect the sample to be representative of all galaxy systems in low density environment. It seems however, that the sample still provide enough information that some general conclusions might be drawn, in particular concerning the different behaviours of early-type and late-type galaxies in pairs and groups detected in low density environments.

The main data for the 11 confirmed SSSGs investigated here are presented in 1. We have checked the NED for SSSGs neighbours with known redshift out to a distance of $600h_{100}^{-1}$ kpc and $1h_{100}^{-1}$ Mpc respectively (see Table 1). Though obtained from a data base which is clearly not complete, this information is listed to allow a quantitative first order approximation of the galaxy density around each SSSG. All SSSGs are in environments including less than 10 galaxies within a projected area of $1h_{100}^{-1}$ Mpc and a redshift range of ± 1000 km s⁻¹ from the SSSG center. This is used to argue that SSSGs are indeed in a low density environment, ranging from completely isolated to that typical for loose groups.

The observed sample contains additionally 2 SSSGs which have not been investigated in detail, namely CGCG 054-011 ($\alpha(2000)$ 17 15 08.7 $\delta(2000)$ 08 27 22) and CGCG 054-013 ($\alpha(2000)$ 17 15 11.9 $\delta(2000)$ 08 25 35). According to literature data, they satisfied our selection criteria. However, our spectroscopic investigation revealed that they are an optical alignment having $V_{hel}=10001\pm 11$ km s⁻¹ and $V_{hel}=6444\pm 11$ km s⁻¹ respectively. They are no further considered in the paper.

3. Observation and reduction

Grey-scale images of the SSSG sample obtained with the 0.91m Dutch telescope at ESO La Silla are presented in Figure 1.

3.1. Spectroscopic observations and analysis

Long-slit spectra were acquired at ESO 1.52m telescope at La Silla equipped with a Boller & Chivens Cassegrain spectrograph during an observing run in 1996. The spectra

of the SSSG member galaxies were obtained in the wavelength region $3500 \leq \lambda \leq 11000$ Å with a dispersion of $3.69 \text{ Å pixel}^{-1}$. The slit (slit width $2''$) has been oriented along the line connecting the nuclei of two of the SSSG members in order to optimize exposure times. The detector used was a FA 2048L UV-coated CCD (ESO CCD #15.) The members which have been observed within each SSSG are reported in Table 2. The observing log of the observations is given in Table 3.

The spectra were calibrated with the ESO-MIDAS² software package using standard procedures for bias subtraction and flat field correction. Artifacts produced by cosmic ray events were removed by applying a filtering algorithm. Wavelength calibration was performed on the frames by fitting a third order polynomial, using as reference the helium-argon spectrum taken before each object spectrum. The spectra were flux calibrated with the IRAF³ package KPNOSLIT. This procedure included the airmass and extinction corrections using standard stars and the atmospheric extinction coefficients. The flux calibrated, de-redshifted spectra are presented in Figure 2.

Heliocentric systemic velocities have been obtained through a cross-correlation technique using the IRAF task CROSSCOR or through the interpolation of emission (or absorption) lines with a single gaussian fit, when the cross-correlation yielded no results because of low signal-to-noise absorption line data. Our redshift measurements were compared with data available in the literature. We found an average systemic velocity difference of 84 km s^{-1} with a standard deviation of 132 km s^{-1} .

The integrated flux of the prominent emission lines ($\text{H}\beta$, $[\text{OIII}] \lambda 4959\text{Å}$, $\lambda 5007\text{Å}$, $\text{H}\alpha$, $[\text{NII}] \lambda 6548\text{Å}$, and $[\text{SII}] \lambda 6717\text{Å}$) was measured using an interactive gaussian fitting procedure and is reported in the Table 4.

3.2. Photometric observations and analysis

Imaging was carried out with the 0.91m Dutch telescope at ESO, La Silla, Chile, during a single run in 1996. Bessel *R* band images were obtained under homogeneous observing conditions. The detector employed was a SITe 512×512 pixel CCD (ESO CCD #33) with a scale of $0.442'' \text{ pixel}^{-1}$ yielding a field of view of $3'.8 \times 3'.8$. The image cleaning, dark

²ESO-MIDAS is developed and maintained by the European Southern Observatory.

³IRAF is distributed by the National Optical Astronomy Observatories, which are operated by the Association of Universities for Research in Astronomy Inc., under cooperative agreement with the National Science Foundation.

and bias subtraction, flat-fielding, cosmic ray removal and the final calibration and image manipulation were performed using the ESO-MIDAS software package.

Standard stars used for calibration purposes were obtained in the same instrumental set-up in the fields of PG1633+099 (4 stars), SA 110 (4 stars), Markarian A (4 stars), T-Phe (3 stars). Each of these fields contains several calibration stars, avoiding the crowding problem typical of fields surrounding globular cluster areas. We used the standard photometric transformation equations tailored to the ESO (La Silla) system of extinction coefficients.

Ellipses were fitted by weighted least squares to the isophotes of the SSSG member galaxies using the IRAF ISOPHOTE package (Jedrzejewski 1987) within STSDAS. Surface brightness, position angle and ellipticity profiles together with the Fourier-coefficients to quantify the deviations of the isophotes from pure ellipses were derived for the early-type members. The b_4 coefficient is in particular used to analyze the boxiness/diskiness of the early-type galaxies. In the case of late-type disk galaxies only the surface brightness, ellipticity and position angle profiles are used for the further analysis. Furthermore, in order to avoid artifacts due to the presence of spiral arms and bright HII regions, the ellipse fitting procedure was repeated iteratively until a satisfactory representation of the stellar disk component could be achieved. Using the parameters extracted from the surface photometry, a smooth model of the galaxy has been produced and subtracted from the original image in order to evidence faint structures (Schweizer 1992) possibly connected to on-going/past interaction episodes. The profiles outside the seeing dominated central region are presented in Figures 3 and 4. The observing log and the results from surface photometry are summarized in Table 5. Further, the imaging data was used to establish morphological types for those galaxies, where either no classification is available in NED or the present data reveal a morphology in conflict with NED.

4. Results and Comments on individual objects

In this section we comment about particular features of the SSSGs in the sample and on individual galaxies in the SSSGs recovered from surface photometry and spectroscopy.

SSSG 1 The galaxies are members of WBL 637 (White et al. 1999) which is formed by 4 objects of which SSSG1a and SSSG1b are WBL members 002 and 003, respectively. The WBL determination agrees with our redshift study of possible neighbours as shown in Table 1. Both galaxies have early-type morphology. No emission lines are detected in the spectra of both members. Surface photometry of SSSG 1a reveals an early-type disk system seen nearly edge-on. The stellar disk component appears prominent both in the residual image

and the b_4 profile. SSSG 1b is an elliptical galaxy, which shows a moderate, $\approx 10^\circ$, isophote twist, while the ellipticity increases up to ≈ 0.4 . The Fourier coefficient b_4 reveals a small disk component in the range $4'' \leq r \leq 10''$. The presence of the inner stellar disk is also visible in the surface brightness profile. A diffuse structure is present in the residual image. A plethora of dwarf galaxies is detected nearby SSSG 1b. According to the systemic velocities of SSSG 1a and SSSG 1b, we suggest that the objects are physically paired, although we do not notice obvious signatures of interaction. Spectra, shown in Figure 2, are typical of their morphological class.

SSSG 2 This system is a chain of 4 bright galaxies with a systemic velocity difference less than 140 km s^{-1} . Galaxies in this poor association appear also in the WBL catalog (WBL 642). The chain, from the north to the south, is composed of a Sc face-on spiral with multiple arms (SSSG 2d), followed by two early-type galaxies (SSSG 2b, SSSG 2a). The fourth member (SSSG 2c) is a face-on Sc spiral with two prominent open arms but diffuse patchy areas, some of them marking incipient spiral arms.

SSSG 2a (E/S0) shows a rising ellipticity profile and a positive (up to 4%) Fourier coefficient b_4 indicating the presence of an inner stellar disk. No emission lines are detected. Three faint objects (Figure 1b) are nearby to SSSG 2a in projection, two north and one south of it. The northern object of the two is compact, with faint and narrow emission lines. The $\text{H}\alpha/[\text{NII}] \lambda 6583\text{\AA}$ line ratio indicates a Seyfert 1-like AGN. The radial velocity is $2159 \pm 54 \text{ km s}^{-1}$. The second object is blue, with faint and narrow lines. The radial velocity is $2165 \pm 262 \text{ km s}^{-1}$. The southern object is an edge-on disk galaxy with a radial velocity of $6717 \pm 59 \text{ km s}^{-1}$ suggesting a physical association with SSSG 2a. SSSG 2b (E/S0) shows a low ellipticity $\epsilon \approx 0.2$ and a strong isophotal twist of $\approx 120^\circ$. The Fourier coefficients a_4 and b_4 indicate the presence of a stellar disk component in the inner part of the galaxy. SSSG 2c is a face-on late-type spiral galaxy with multiple arms of which two dominate. Surface brightness and position angle profiles reveal the presence of a small exponential bar component in the region $4'' \leq r \leq 13''$. The residual image shows a number of smaller spiral arms. SSSG 2d is a late-type face-on spiral with flocculent arms. Some of them mark incipient spiral arms. A number of HII regions appears in the residual image after subtracting a smooth galaxy model. SSSG 2c and SSSG 2d show emission lines ratios characteristic of HII regions.

A number of faint galaxies is noted in the immediate surroundings of the bright galaxies. Of particular interest is a faint disk galaxy (Figure. 1c) which is detected between SSSG 2b and SSSG 2d. The object shows strong and narrow emission features in the spectrum, with line ratios consistent with typical HII regions. The measured radial velocity is $6626 \pm 64 \text{ km s}^{-1}$ in agreement with the systemic velocity of SSSG 2.

SSSG 3 The isolated multiplet consists of 4 confirmed galaxies with 5 possible neighbours within 1 Mpc. The two early-type member galaxies of the multiplet are seen nearly edge-on. SSSG 3a has been classified as E6 according to NED. However, the surface brightness profile reveals a bulge and a stellar disk component suggesting therefore an E/S0 type. The presence of a stellar disk component is further confirmed by an overall positive b_4 coefficient and evidenced in the residual image. SSSG 3b has a constant position angle profile and the ellipticity increases up to 0.6. The surface brightness profile also shows the presence of a bulge and a disk component supporting the classification of S0:Sp from NED. The latter is also revealed in the residual image. The galaxy is surrounded by faint objects possibly dwarf galaxies. No emission lines are detected in SSSG 3a and SSSG 3b as expected from their morphological class. There are no morphological signatures of interactions detected between the galaxies.

SSSG 4. The pair also known as KPG 551 (Karachentsev 1972) shows pronounced signatures of interaction. The southern object SSSG 4a appears strongly interacting and is of irregular type. The northern object SSSG 4b, which is classified as SAB pec, shows an arc-like tail/arm extending to the northeast of the galaxy. This structure contains numerous HII regions (Junqueira, de Mello, & Infante 1998). We measured a virtually null systemic velocity difference as reported in the literature. Both members show prominent emission lines. The apparent peculiarities of this isolated pair prevent us to perform a detailed surface photometry. Between the SSSG 4a and SSSG 4b there is a faint object, with narrow emission lines. No absorption lines were detected. The measured radial velocity is 6954 ± 127 km s⁻¹.

SSSG 5 The isolated pair ($\Delta V=104$ km s⁻¹) is composed of an edge-on lenticular and a grand design spiral galaxy. The S0 galaxy SSSG 5a shows a two component surface brightness profile consisting of a bulge and stellar disk component. The ellipticity profile rises up to 0.5 and the position angle profile is nearly constant at $\approx 80^\circ$. The Fourier coefficient b_4 further evidences the disk component ($\approx 8\%$). No emission lines are detected in the spectrum. The presence of strong spiral arms in SSSG 5b prevented a detailed surface photometric analysis. The galaxy spectrum shows faint emission lines.

SSSG 6 The members of the multiplet appear to be quite separated from each other. SSSG 6 is composed of three late-type members: SSSG 6a, seen almost face-on, SSSG 6b and a third object, for which no spectroscopic data are available and which is seen almost edge-on. The derived $H\alpha/[NII] \lambda 6583\text{\AA}$ line ratio for the nucleus of SSSG 6a suggests a Seyfert 1-like AGN. This galaxy is also detected by IRAS (IRAS 00000-0359). The presence of strong spiral arms in SSSG 6a prevent us to perform a detailed surface photometry. A number of HII regions appears in the residual image after subtraction of a smooth model galaxy.

SSSG 6b appears to be distorted with two inner main arms and outer arms completely decoupled. The difference of their systemic velocities is $\approx 200 \text{ km s}^{-1}$ suggesting a physical association.

SSSG 7 The pair is composed of an edge-on lenticular with a thick disk and an early spiral galaxy with very thin spiral arms showing patchy HII regions. The systemic velocity difference between the members is only $\approx 70 \text{ km s}^{-1}$. SSSG 7a shows a rising ellipticity and a constant position angle profile. The b_4 profile indicates a strong (8%) disk component. The photometric data are influenced by a bright star in the vicinity. No spiral arm structure is visible suggesting therefore an S0 type instead of the classification as S? in the NED. SSSG 7b shows faint spiral arms after subtraction of a smooth model galaxy. These arms are more reminiscent of a sort of shell structure created by weak interaction (Thomson 1991; Weil & Hernquist 1993) rather than typical spiral arms. The $H\alpha$ intensity is approximately similar to that of [NII] in the galaxy center which indicates the presence of a strong $H\alpha$ component in absorption. The $H\alpha$ /[NII] $\lambda 6583\text{\AA}$ line ratio indicates an AGN of Seyfert 1 type.

SSSG 8 The loose pair consists of two barred spirals seen almost face-on. The imaging data reveal a population of faint objects, possibly dwarf galaxies, surrounding the bright SSSG members. A spectrum was obtained only for the SSSG 8b, which reveals emission lines typical for HII regions.

SSSG 9 The triplet is composed of an unperturbed elliptical and two spiral galaxies. SSSG 9a is a face-on spiral showing multiple arm structure, a small bulge and a prominent disk component. The analysis of the surface brightness profile reveals the presence of an elongated component (possibly a bar component) in the range $10'' \leq r \leq 20''$. The spiral arms are very prominent with a number of large HII regions particularly in the southern arm. SSSG 9b is an apparently undisturbed E0. A spectrum was obtained of the elliptical (SSSG 9b) and the brighter spiral galaxy (SSSG 9a). The difference of the systemic velocities between these two galaxies is 122 km s^{-1} . It is noticeable that the stellar and gas components in SSSG 9a differ in the systemic velocity of about 80 km s^{-1} . The systemic velocity of the gas component is closer to the systemic velocity of SSSG 9b.

SSSG 10 Pierfederici, Rampazzo & Reduzzi (2000) performed a photometric study of the pair which appears completely damaged by the encounter. They report that a complex system of debris extend from the galaxy in south-east direction with intense knots. SSSG 10a is of irregular shape shows strong and narrow emission lines in the spectrum. SSSG 10b is a typical S0, with a dust lane in the center and appears slightly damaged by the encounter in the eastern outer part. The line ratio ($H\alpha$ /[NII] $\lambda 6583\text{\AA}$) < 1 of the SSSG 10b is consistent with that of typical Seyfert galaxy, no [OIII] $\lambda 5007\text{\AA}$ emission is detected.

SSSG 11 The pair does not present evident signatures of interaction as also reported by Pierfederici, Rampazzo & Reduzzi (2000). SSSG 11a is a late-type spiral seen edge-on. Strong emission lines are detected in the spectrum. Also absorption lines are present, but they appear very faint. The northern member, SSSG 11b, is a faint spiral. The spectral features are too faint to be further analyzed.

5. Properties of the morphological classes

5.1. Properties of early-type galaxies

The early-type galaxies of the SSSG sample have been searched for the presence of fine structures, using the scheme developed by Schweizer (1992). However, no significant structures could be detected. This may indicate that either these galaxies remained undisturbed during recent interactions within the SSSG or the interactions occurred only on small scale. Such events could be mass accretions of (gas-rich) dwarf galaxies resulting in kinematically decoupled components which are frequently observed in early-type galaxies. The presently available observational material however has not sufficient resolution to answer this question.

The Hamabe–Kormendy relation HK87 (Hamabe & Kormendy 1987) is a useful tool to study distributions of early-type galaxies using the classification by Capaccioli et al. (1992), hereafter CCD92, in ordinary and bright classes. Bright galaxies are defined as those having $M_B < -19.3$ and $R_e > 3$ kpc ($H_0=70$ km s⁻¹ Mpc⁻¹) while $\mu_e=2.94\log R_e + 20.75$ traces the HK87 relation. CCD92 show that ordinary galaxies do not tend to distribute along the HK87 relation but fill the plane for $R_e < 3$ kpc. The ordinary galaxy class is considered as a sort of “genetic variety” since it contributes to generate bright galaxies through merging processes (Navarro 1990). In order to transform our data from R band to B band we adopt a $(B-R) = 1.5$, i.e. the color of a SSP of solar metallicity ($Z=0.02$) and of an age of 13–15 Gyr. Figure 5 shows the $\mu_e - \log R_e$ plane. The vast majority of our objects resides in the range of ordinary galaxies. This is not the general case of galaxies in low density environments as shown by Rampazzo et al. (2000). They noticed also that there is a number of bright galaxies well below the relation. These latter have been interpreted as a transient phase since they include strongly interacting members. These galaxies completely lack in our sample. This may suggest that SSSGs are either accordant redshift unrelated galaxies or that they are still in a stage of pre-coalescence and have not yet produced the bright merger remnants.

5.2. Properties of spiral galaxies

The late-type galaxies of the SSSG sample show clear signatures of on-going interaction in contrast to the early-types. Following the classification of Elmegreen & Elmegreen (1987) (see Table 6 for classification) most spiral galaxies belong to the grand design class typically found in the densest group environments. At the same time, a significant number of disk galaxies is found in comparatively low-density environments as suggested by the rather small percentage of barred galaxies present in the sample if compared with those detected in binary samples by Elmegreen & Elmegreen (1982) and Reduzzi & Rampazzo (1995). A large fraction of spirals, which are not seen edge-on, show open arms indicating an on-going interaction. According to Noguchi & Ishibashi (1986) models, open arms develop in the very early phases of an encounter. Star formation rate reaches the maximum value of about 8 times as large as the pre-encounter value at about 3×10^8 years after the perigalactic passage of the perturber. In this context we suggest that our multiplet SSSGs could be early phases in the hierarchical assembling process.

The emission line spectra were used to study the ionisation mechanisms. The emission line intensity ratios, as defined by Veilleux & Osterbrock (1987), $[\text{OIII}]/\text{H}\beta$ vs. $[\text{NII}]/\text{H}\alpha$ and $[\text{OIII}]/\text{H}\beta$ vs. $[\text{SII}]/\text{H}\alpha$ of the sample galaxies are plotted in Figure 6. Veilleux & Osterbrock (1987) defined the intrinsic flux ratio for HII region-like objects $I(\text{H}\alpha)/I(\text{H}\beta) = 2.85$ and adopt for the intrinsic ratio of AGNs $I(\text{H}\alpha)/I(\text{H}\beta) = 3.1$. The values of the flux ratio in the sample are found to be generally bigger and using the two definitions of Veilleux & Osterbrock (1987), the value of the flux intensity of $\text{H}\beta$ is corrected. This is attributed to the fact that the $\text{H}\beta$ flux is underestimated due to the presence of an absorption line component. The new value of the flux intensity of $\text{H}\beta$ is used to compute new $[\text{OIII}]/\text{H}\beta$ vs. $[\text{NII}]/\text{H}\alpha$ and $[\text{OIII}]/\text{H}\beta$ vs. $[\text{SII}]/\text{H}\alpha$ ratios (see errorbars in Figure 6). Figure 6 shows that late-type galaxies in the sample are dominated by photoionisation: all objects lie in the region of the diagram, which is dominated by HII-regions. This is the case also for morphologically peculiar galaxies, as e.g. SSSG 4b and SSSG 6b and even strongly distorted galaxies, e.g. SSSG 4a and SSSG10a.

Star formation rates (SFR) were calculated, using the calibration between SFR and $\text{H}\alpha$ fluxes adopted by Kennicutt (1998) (see Table 5):

$$SFR(M_{\odot}\text{yr}^{-1}) = 7.9 \times 10^{-42} \times L_{\text{H}\alpha}(\text{ergs}^{-1})$$

Table 4 (column 12) collects the SFR for the disk galaxies of the sample. Most disk galaxies (9 out of 14) can be considered “normal”, with star formation rates up to $8 M_{\odot} \text{yr}^{-1}$. The remaining 5 objects have a significantly higher star formation rate. However only one exceeds the value of $50 M_{\odot} \text{yr}^{-1}$, which indicate a major starburst phenomenon. It is worth

remarking that the 5 disk galaxies presenting the higher SFR are hosted in the more isolated SSSGs of the sample (see Table 1), and in SSSGs containing only spiral galaxies.

6. Summary

In this paper we have studied 19 members in 11 SSSGs and presented their photometric and spectroscopic properties. Our selection criteria have included small systems ranking from isolated pairs (KPG 551, RR23 and RR45) with no neighbours of similar luminosity to poor groups in low density environment. The groups are high density configurations and some of them are catalogued in the literature as nearby poor clusters, as in the case of SSSG 1 (WBL 637) and SSSG 2 (WBL 642).

Although the relatively small number of objects studied so far does not allow to draw statistically significant conclusions some trends can still be pointed out. Early-type galaxies in SSSGs, even those which are found in more compact multiplets, do not show relevant signatures of interaction. The lack of evidence of early-type galaxies being the result of major merger events is a feature in common with HCGs, which have a low fraction of merging candidates and no evidence of enhanced far-infrared emission (Zepf & Whitmore 1991; Zepf 1993; Verdes-Montenegro et al. 1998). Further, the early-type galaxies of our sample do not show fine structure. This is not surprising, indeed Reduzzi, Longhetti & Rampazzo (1996) found that e.g. shell structures are found four times less frequently in interacting pairs than in isolated objects of the same class. This may be attributed to two causes. First, none of our early-type members is suffering or has recently suffered a strong interaction episode. Most of our early-type members have a disk component or are disky according to the shape parameter b_4 which is often larger than 2%. Second, the galaxies suffer “weak” but multiple interactions that are likely to destroy shell structures (Thomson & Wright 1990).

At variance with early-type galaxies spirals displaying patterns typical of ongoing interaction and high star formation rate are found in SSSGs. These SSSGs are the most isolated in the sample and additionally are the only ones displaying a total spiral population. This finding confirms previous results from studies of classical pairs in the Karachentsev (1972) catalog (Xu & Sulentic 1991) and pairs catalogs in the southern hemisphere (Combes et al. 1994) reporting significant enhancements of star formation due to the infall of fresh gas triggered by the interaction. At the same time the lack of evidence for enhanced star formation in spirals in the densest SSSGs agrees with previous results on HCGs (Sulentic & de Mello Rabaca 1993; Verdes-Montenegro et al. 1998) and on UZC-CGs (Kelm, Focardi & Zampieri 2003). Neither our SSSGs which are strongly interacting nor members in multiplets do show unambiguously the presence of nuclear activity.

Further steps in the study of our sample of SSSGs are planned/on-going. Among these, to obtain X-ray imaging and a deeper mapping of SSSGs through wide field imaging data which will permit a better definition of their environment. The spectroscopic information are then a necessary information to understand the significance of the population of faint galaxies accompanying SSSGs in their evolution. This will allow to test directly small scale substructure formations theories. High resolution spectroscopy will give the necessary information (line-strength indices etc.) about single members evolution.

We are deeply indebted to Dr. Luca Reduzzi which performed observations. RR acknowledges the kind hospitality of the Institut für Astronomie der Universität Wien during the preparation of the paper. LT and WWZ acknowledge the support of the Austrian Science Fund (project P14783). The research has made use of the NASA/IPAC Extragalactic Database (NED) which is operated by the Jet Propulsion Laboratory, California Institute of Technology, under contract with National Aeronautics and Space Administration.

REFERENCES

- Barnes, J. 1996, Galaxies: Interactions and Induced Star Formation, Saas-Fee Advanced Course 26, 275
- Combes, F., Prugniel, P., Rampazzo R. & Sulentic, J. W. 1994, A&A, 281, 725
- Capaccioli, M., Caon, N., D’Onofrio, M. 1992, Structure, Dynamics and Chemical Evolution of Early-Type Galaxies, ESO-EIPC Workshop, Danziger J. et al., 43 (CCD92)
- Coziol, R., Iovino, A. & de Carvalho, R. R. 2000, AJ, 120, 47
- Diaferio, A. Geller, M.J. & Ramella, M. 1994, AJ, 107, 868
- Elmegreen, D. M. & Elmegreen, B. G. 1982, MNRAS, 201, 1021
- Elmegreen, D. M. & Elmegreen, B. G. 1987, ApJ, 314, 3
- Focardi, P. & Kelm, B. 2002, A&A, 391, 35
- Forman, W. & Jones, C. 1982, ARA&A, 20, 547
- Governato, F., Tozzi, P. & Cavaliere, A. 1996, ApJ, 458, 18
- Haynes, M.P., Giovanelli, R. & Chincarini, G. 1984, ARA&A, 22, 445

- Hamabe, M. & Kormendy, J. 1987, Structure and Dynamics of elliptical Galaxies, IAU Symp. No. 127 (Princeton), ed. T. de Zeeuw, Dordrecht: Reidel, 379: (HK87)
- Henricksen M. & Cousineau, S. 1999, ApJ, 511, 595
- Hickson P. 1997, ARA&A, 35, 357
- Huchra, J.P, Geller, M.J., Clemens C.M., Tokarz S.P. & Michel A. 1992, Bull. Inf. CDS, 41,31
- Jedrzejewski, R. 1987, MNRAS 226, 747
- Junqueira, S., de Mello, D. F. & Infante, L., 1998, A&AS, 129, 69
- Karachentsev, I. D. 1972, Catalogue of isolated pair of galaxies in the northern hemisphere, Soob-shch. Spets. Astrofiz. Obs. 7,3
- Keel, W. C. 1996, AJ, 111, 696
- Kennicutt, R. C. 1996, Galaxies: Interactions and Induced Star Formation, Saas-Fee Advanced Course 26, 1
- Kennicutt, R.C. 1998, ARA&A, 36, 189
- Kelm, B., Focardi, P. & Palumbo, G.G.C. 1998, A&A, 335, 912.
- Kelm, B., Focardi P. & Zampieri, A. 2003, Galaxy Evolution III: From simple Approaches to self consistent Models, ed. G. Hensler, Kluwer Academic Publisher, in press
- Laurikainen, E. & Salo, H. 1995, A&A293, 683
- Longhetti, M., Rampazzo, R., Bressan, A. & Chiosi, C. 1998a, A&A, 130, 251
- Longhetti, M., Rampazzo, R., Bressan, A. & Chiosi, C. 1998b, A&A, 130, 267
- Longhetti, M., Bressan, A., Chiosi, C. & Rampazzo, R. 1999, A&A, 345, 519
- Longhetti, M., Bressan, A., Chiosi, C. & Rampazzo, R. 2000, A&A, 353, 917
- Monaco, P., Giuricin, G., Mardirossian, F., Mezzetti, M. et al. 1994, ApJ, 436, 576
- Moore, B., Katz, N., Lake, G., Dressler, A. & Oemler, A., Jr. 1996, Nature, 379, 613
- Mulchaey, J. S. & Zabludoff, A. I. 1999, ApJ, 514, 33
- Mulchaey, J. S. 2000, ARA&A, 38, 289

- Navarro, J. F. 1990, MNRAS, 242, 311
- Noguchi, M. & Ishibashi, S. 1986, MNRAS, 219, 305
- Pierfederici, F., Rampazzo, R. & Reduzzi, L. 2000, *Astrophys. Lett.*, Vol. 40, 84.
- Ponman, T. J., Bourner, P. D. J., Ebeling, H. & Böhringer, H. 1996, MNRAS, 283, 690
- Rafanelli, P., Violato, M. & Baruffolo, A. 1995, AJ, 109, 1546
- Rampazzo, R. & Sulentic, J. W. 1992, A&A259, 43
- Rampazzo, R., D’Onofrio, M., Bonfanti, P., Longhetti, M. & Reduzzi, L. 2000, *Astrophys. Lett.*, Vol. 40, 63
- Reduzzi, L. & Rampazzo, R. 1995, *Astrophys. Lett.*, Vol. 30., 1: RR95
- Reduzzi, L., Longhetti, M. & Rampazzo, R. 1996, MNRAS, 282, 149
- Schweizer, F. 1992, *Structure, Dynamics and Chemical Evolution of Early-type Galaxies*, ESO–EIPC Workshop, Danziger et al., 651
- Schweizer F. 1996 *Galaxies: Interactions and Induced Star Formation*, Saas–Fee Advanced Course 26, 105
- Struble, M. F. & Rood, H. J. 1999, ApJS, 125, 35
- Sulentic J.W. & de Mello Rabaca, D. 1993, ApJ, 410 520
- Thomson, R. C. & Wright, A. E. 1990, MNRAS, 247, 122
- Thomson, R. C. 1991, MNRAS, 253, 256
- Trinchieri, G. & Rampazzo, R. 2001, A&A, 374, 454
- Veilleux, S. & Osterbrock D. E. 1987, ApJS, 63, 295
- Verdes–Montenegro, L., Yun, M. S., Perea, J., del Olmo, A. & Ho, P. T. P. 1998, ApJ, 497, 89
- Weil, M.L. & Hernquist, L. 1993, ApJ, 405, 142
- Xu, C. & Sulentic J. W. 1991, ApJ, 374, 407
- White, R. A., Blinton, M., Bhavsar, S. P. et al. 1999, AJ, 118, 2014

Zabludoff, A. & Mulchaey, J. 1998, ApJ, 498, L5

Zepf, S. E. & Whitmore, B. C. 1991, ApJ, 383, 542

Zepf, S. E. 1993, ApJ, 407, 448

Fig. 1.— Bessel R band images of the SSSG sample. Top row: SSSG 1 (A), SSSG 2 southern part (B), SSSG 2 northern part (C), SSSG 3 (D), central row: SSSG 4 (E), SSSG 5 (F), SSSG 6 southern part (G), SSSG 6 northern part (H) and bottom row: SSSG 7 (I), SSSG 8 (J), SSSG 9 (K). North is on the top, East to the left. The field of view is $3.8' \times 3.8'$.

Fig. 2.— Spectral energy distribution for SSSG members: early-type galaxies (top row, left and central panel, late-type galaxies (top row, right panel and bottom row all panels) Main features are indicated. Spectra have been de-redshifted to the rest frame. The galaxy spectra are displaced by a constant value of $5 \times 10^{-14} \text{ erg cm}^{-2} \text{ s}^{-1} \text{ \AA}^{-1}$, from each other for clarity.

Fig. 3.— Surface photometry of early-type SSSG members: SSSG 1a, SSSG 1b, SSSG 2a (top row), SSSG 2b; SSSG 3a, SSSG 3b (center row); SSSG 5a, SSSG 7a, SSSG 9b (bottom row). Each panel displays surface brightness (R mag arcsec^{-2}), ellipticity ($1-b/a$), position angle, and Fourier coefficients a_4 and b_4 as a function of radius

Fig. 4.— Surface photometry of late-type SSSG members: SSSG 2c, SSSG 2d, SSSG 5b (top row), SSSG 6a; SSSG 6b, SSSG 7b (center row); SSSG 8b, SSSG 9a (bottom row). Each panel displays surface brightness (R mag arcsec^{-2}), ellipticity ($1-b/a$), position angle as a function of radius

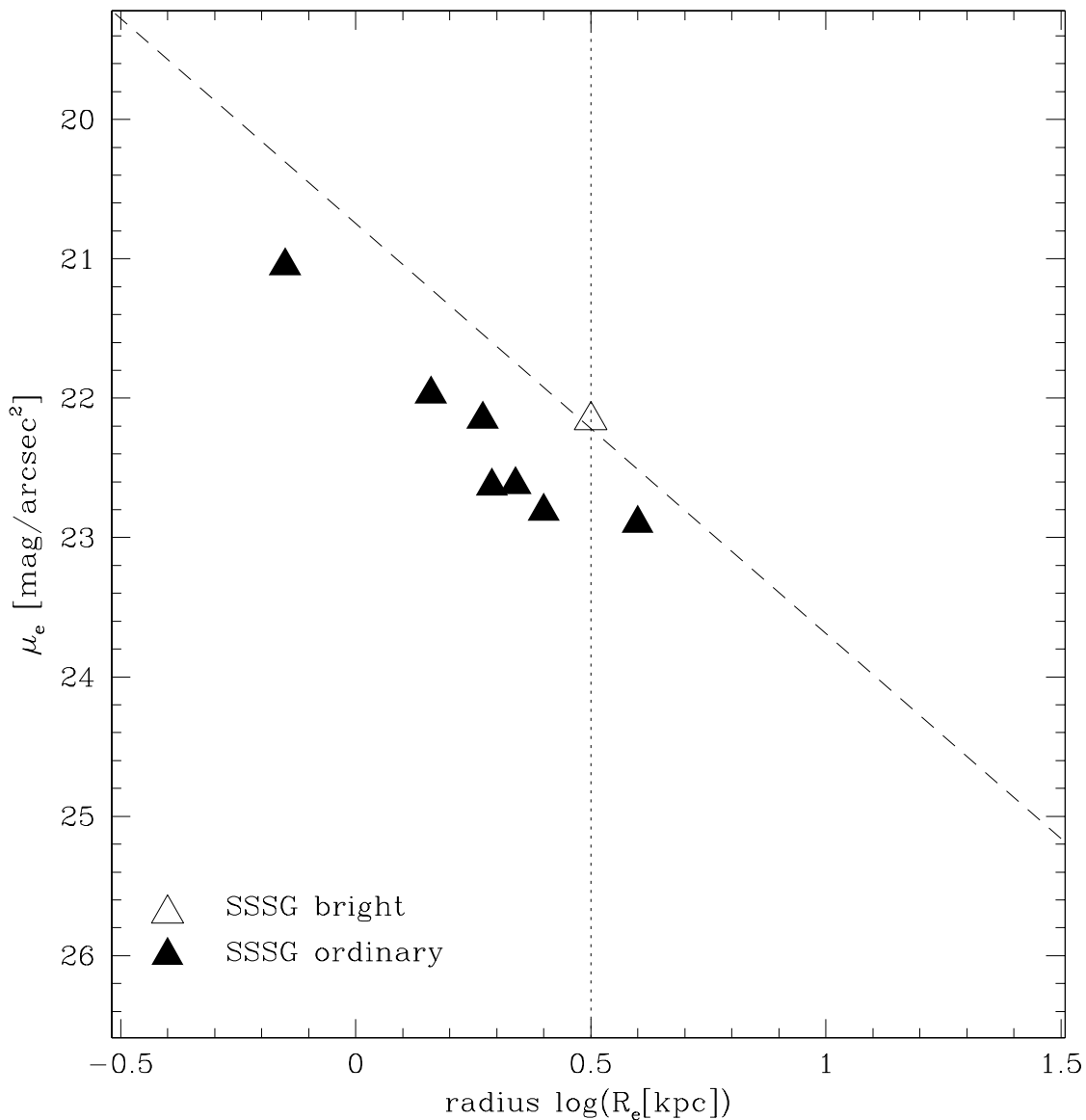


Fig. 5.— Effective radius, in kpc, versus the effective B surface brightness. The diagonal long-dashed line marks the HK87 relation, differentiating between bright and ordinary galaxies. The vertical dotted line at $\log R_e=0.5$ i.e. 3 kpc ($H_0=70 \text{ km s}^{-1} \text{ Mpc}^{-1}$) separates luminous from ordinary ellipticals according to Capaccioli et al. (1992)

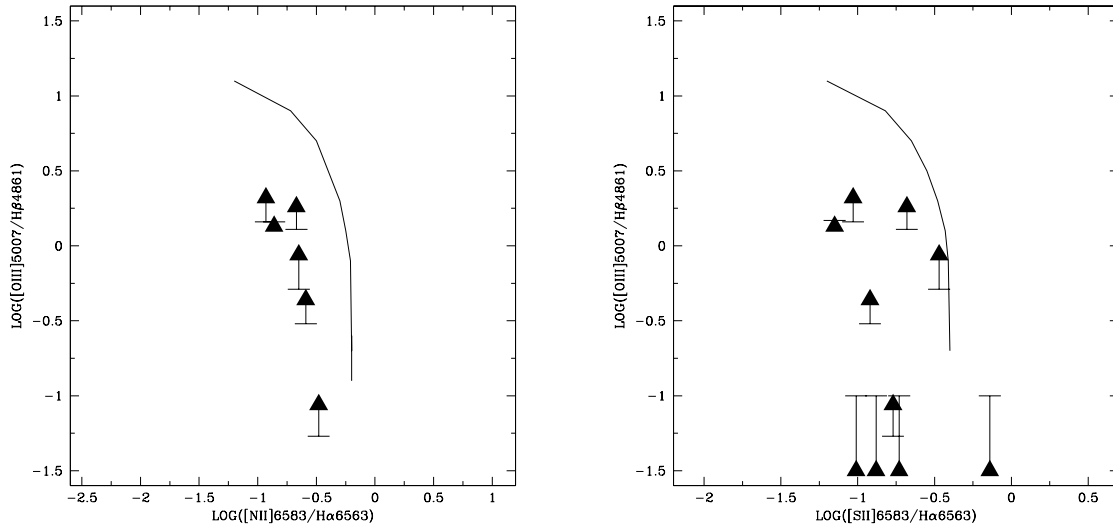


Fig. 6.— $[\text{OIII}]/\text{H}\beta$ vs. $[\text{NII}]/\text{H}\alpha$ (left panel) and $[\text{OIII}]/\text{H}\beta$ vs. $[\text{SII}]/\text{H}\alpha$ (right panel) intensity ratios (solid curve divides AGNs from HII region-like, same scale as has been used in Veilleux & Osterbrock, 1987).

Table 1. Parameters and environment of SSSG sample.

SSSG (1)	V_{hel} (2)	n_{CGA} (3)	n_{600kpc} (4)	n_{1Mpc} (5)	σ_v (6)	Notes (7)
1	6588	4	1	5	172	WBL 637
2	6688	4	2	3	113	WBL 642
3	4578	4	0	5	168	
4	5769	2	0	0	2	KPG 551
5	8526	2	0	1	104	
6	6297	3	0	1	132	
7	8824	2	0	0	74	
8	5433	2	1	3	88	
9	4739	3	1	4	108	
10	3630	2	0	0	9	RR23
11	6081	2	1	4	489	RR45

¹SSSG identification

²heliocentric velocity of the group [km s⁻¹]

³number of group members within $r < 200 h_{100}^{-1}$ kpc

⁴number of group members within $r < 600 h_{100}^{-1}$ kpc

⁵number of group members within $r < 1 h_{100}^{-1}$ Mpc

⁶velocity difference of the pair [km s⁻¹]

⁷other group identifications

Table 2. Salient spectroscopic properties of the SSSG members.

SSSG ident.	α (2000)	δ (2000)	other ident.	morphol. Type	V_{hel} km s^{-1}
1a	17 17 25.2	07 41 43	CGCG 054-019	S0	6730±12
b	17 17 33.4	07 39 43	CGCG 054-020	E	6368±13
	17 17 13.3	07 44 29	CGCG 054-018	...	6536 ⁴⁾
	17 17 44.9	07 36 30	UGC 10789	...	6719 ⁴⁾
2a	17 31 55.0	06 29 00	CGCG 055-003	E/S0	6846±13
b	17 31 54.2	06 30 07	CGCG 055-004	E/S0	6687±15
c	17 31 57.0	06 28 09	CGCG 055-005	SBc	6632±174 ²⁾
d	17 31 58.8	06 31 56	CGCG 055-006	Sc	6587±34 ²⁾
3a	20 32 36.7	09 53 02	NGC 6927A	E/S0	4568±191 ²⁾
b	20 32 38.2	09 54 59	NGC 6927	S0:Sp ¹⁾	4344±206 ³⁾
	20 32 50.2	09 55 38	NGC 6928	SB(s)ab ¹⁾	4707 ⁴⁾
	20 32 58.8	09 52 28	NGC 6930	SB(s)ab? ¹⁾	4694 ⁴⁾
4a	20 59 46.9	-01 53 16	UGC 11657	Irr	5768±45 ²⁾
b	20 59 48.3	-01 52 23	UGC 11658	SAB(rs)pec? ¹⁾	5770±7 ²⁾
5a	22 01 01.7	08 06 34	A2158+0752	S0	8474±11
b	22 01 10.8	08 07 32	A2158+0753	S	8578±6 ²⁾
6a	00 02 34.8	-03 42 38	MCG -01-01-024	SB(s)bc? ¹⁾	6448±30 ²⁾
b	00 02 38.5	-03 37 51	MCG -01-01-025	S	6242±12 ²⁾
	00 02 48.7	-03 36 21	MCG -01-01-026	S	6202 ⁴⁾
7a	00 03 22.3	-10 46 14	MCG -02-01-012	S0	8861±11
b	00 03 32.1	-10 44 41	NGC 7808	(R')SA0 ¹⁾	8787±19
8a	01 51 34.0	-08 23 56	MCG -02-05-065	SB	5389±2 ²⁾
b	01 51 27.0	-08 30 20	NGC 0707	(R')SAB(s)0 ¹⁾	5477±2 ²⁾
9a	02 37 34.7	-11 01 34	NGC 1010	SB	4588±11
b	02 37 38.9	-11 00 20	NGC 1011	E0	4754±17
	02 37 49.8	-11 00 39	NGC 1017	S	4876 ⁴⁾
10a	01 14 20.1	-55 24 02	NGC 0454 NED01	Irr	3626±2 ²⁾
b	01 14 25.2	-55 23 47	NGC 0454 NED02	Irr	3635±2 ²⁾
11a	02 06 22.2	-36 18 01	ESO 354- G 036	Sc ¹⁾	6325±17 ²⁾
b	02 06 53.1	-36 27 08	NGC 824	SB(RS)b ¹⁾	5836±10 ²⁾

¹⁾morphological type from NED

²⁾heliocentric velocity is determined from averaged gaussian fits to single emission lines

³⁾heliocentric velocity is determined from averaged gaussian fits to single absorption lines

⁴⁾heliocentric velocity from NED

Table 3. Spectroscopic observations

SSSG (1)	PA (2)	time (3)	objects (4)	SSSG (1)	PA (2)	time (3)	objects (4)	SSSG (1)	PA (2)	time (3)	objects (4)
1	134	30	a, b	5	67	30	a, b	9	41	30	a, b
2	147	30	a, c	6	4	30	a	10		30	a, b
2	30	30	b, d	6	98	30	b	11		30	a
3	11	30	a, b	7	56	30	b				
4	22	30	a, b	8	62	30	b				

¹SSSG identification

²position angle of the slit [deg]

³exposure time [min]

⁴SSSG member galaxies covered by the slit

Table 4. Emission line fluxes and SFRs

SSSG	H β (1)	[OIII]N1 (1)	[OIII]N2 (1)	H α (1)	[NII] (1)	[SII] (1)	$\log \frac{[OIII]}{H\beta}$	$\log \frac{[NII]}{H\alpha}$	$\log \frac{[SII]}{H\alpha}$	H α /H β	SFR (2)
2c	... ³	67.6	37.6	-0.26	8
2d	... ³	25.6	8.8	7.5	...	-0.47	-0.73	...	3
4a	120.0	81.5	250.0	495.0	58.0	54.6	0.32	-0.93	-1.03	4.13	43
4b	85.0	17.5	37.0	348.0	89.4	41.4	-0.36	-0.59	-0.92	4.09	30
5b	25.9	17.1	-0.18	5
6a	... ³	23.2	49.9	16.8	...	0.33	-0.14	...	3
6b	22.8	11.5	20.0	110.0	24.9	37.7	-0.06	-0.65	-0.47	4.82	11
7b	... ³	14.8	16.5	... ³	...	0.05	3
8b	36.1	23.4	21.0	3.1	...	-0.05	-0.88	...	2
9a	29.7	2.0	2.6	137.0	45.2	23.1	-1.06	-0.48	-0.77	4.61	8
9b	... ³	30.3	2.1	-1.15	2
10a	575.0	272.0	769.0	1490.0	204.0	105.0	0.13	-0.86	-1.15	2.6	51
10b	... ³	...	82.8	562.0	566.0	54.6	...	0.003	-1.01	...	19
11a	15.7	27.6	28.7	63.5	13.5	13.4	0.26	-0.67	-0.68	4.04	6

¹Line fluxes are given in units of 10^{-14} erg cm $^{-2}$ s $^{-1}$

²Star formation rate [M_{\odot} yr $^{-1}$]

³Spectral feature in absorption

Table 5. Salient properties from the surface photometry of the SSSG members

SSSG (1)	FWHM (2)	Exp. T. (3)	R_T (4)	M_R (5)	r_e (6)	μ_e (7)	μ_0 (8)
1a	1.4	30	13.13	-20.89	12.30	22.02	18.73
b			13.25	-20.84	7.00	20.66	18.67
2a	1.2/1.4	2×30	13.96	-20.13	4.11	20.65	18.82
b			14.21	-19.92	3.08	20.47	18.60
c			14.15	-19.96	20.29
d			14.30	-19.79	20.70
3a	1.4	30	15.02	-18.21	2.31	19.55	19.02
b			13.91	-19.25	8.39	21.31	18.56
4a	1.8	3×20	13.75	-20.05	20.14
b			13.07	-20.74	20.21
5a	1.2	30	14.83	-19.78	3.74	21.12	19.30
b			15.52	-19.15	20.44
7a	1.4	30	13.19	-21.55	5.47	20.40	18.21
b			12.54	-22.17	12.30	21.89	18.49
8a	1.4	40	14.14	-21.00	19.72
b			13.73	-19.83	19.61
9a	1.4	30	12.82	-20.54	12.29	21.40	19.67
b			13.35	-20.01	6.02	21.00	18.69

¹SSSG and group member galaxy identification

²seeing as measured FWHM of stellar images in the frame[$''$]

³exposure time [min]

⁴apparent total magnitude m_R

⁵absolute total magnitude M_R

⁶effective radius [$''$]

⁷surface brightness $\mu_e(R)$ measured at the effective radius [mag arcsec $^{-2}$]

⁸central surface brightness $\mu_0(R)$ [mag arcsec $^{-2}$]

Table 6. Arm classes of the spiral members.

SSSG #	AC type	Notes
2c	9	bar
2d	3	
5b	12	
7b	8	
8b	12	bar
9a	6	bar

This figure "Tanvuia.fig1.jpg" is available in "jpg" format from:

<http://arxiv.org/ps/astro-ph/0306287v1>

This figure "Tanvuia.fig2.jpg" is available in "jpg" format from:

<http://arxiv.org/ps/astro-ph/0306287v1>

This figure "Tanvuia.fig3.jpg" is available in "jpg" format from:

<http://arxiv.org/ps/astro-ph/0306287v1>

This figure "Tanvuia.fig4.jpg" is available in "jpg" format from:

<http://arxiv.org/ps/astro-ph/0306287v1>